

# Role of Splitter Plates in Modifying Cylinder Wake Flows

M. A. Z. Hasan\* and M. O. Budair\*

King Fahd University of Petroleum & Minerals, Dhahran 31261, Saudi Arabia

The effects of a splitter plate as well as the gap  $g$  between the splitter plate and the trailing edge of a cylinder on the frequency characteristics of the cylinder were investigated over a Reynolds number  $Re_D$  range of  $1.2 \times 10^4$  to  $2.4 \times 10^4$ . A splitter plate attached at the trailing edge of the cylinder decreased the frequency of the peak observed in the velocity spectrum compared with the global shedding frequency of the wake for the cylinder alone. For  $g/D \leq 3$ , the frequency of dominant spectral peak remained less than the global shedding frequency, presumably controlled by the local shear layer instability frequency, whereas for  $g/D > 3$ , the frequency increased to the global shedding frequency. It has been shown that the detailed pressure distribution around the cylinder can be used to predict the increase or decrease of the frequency. For the first time, a coupling between the local shear layer instability and the wake instability on the frequency characteristics of such a flow has been suggested.

## Nomenclature

- $C_p$  = pressure coefficient,  $2(P - P_\infty) / (\rho U_\infty^2)$   
 $D$  = cylinder diameter or side of the square cylinder  
 $D_p$  = maximum width of the cylinder normal to flow  
 $f$  = frequency, Hz  
 $g$  = gap between the cylinder and the splitter plate  
 $L$  = length of the splitter plate  
 $l$  = length of the cylinders  
 $P$  = pressure at any point  
 $P_\infty$  = freestream pressure  
 $Re_D$  = Reynolds number,  $U_\infty D / \nu$   
 $St_D$  = Strouhal numbers,  $fD / U_\infty$   
 $U_\infty$  = freestream longitudinal mean velocity  
 $x$  = downstream distance from the trailing edge of the cylinder  
 $y$  = transverse distance from the  $x$  axis  
 $\alpha$  = angle of incidence  
 $\nu$  = kinematic viscosity of air  
 $\rho$  = density of air

## I. Introduction

IT has been demonstrated by a number of experimental studies that a splitter plate mounted rigidly behind a circular cylinder can significantly modify the wake flow characteristics. Roshko<sup>1,2</sup> was the first to study the effect of splitter plates in the wake of a circular cylinder at a  $Re_D$  of  $1.45 \times 10^4$ . He showed that a splitter plate of length  $L = 5D$  in contact with the cylinder suppressed the periodic vortex formation and reduced the pressure drag by approximately 63% of the value for the cylinder alone. For a splitter plate with  $L/D = 1.14$ , the vortex formation was not suppressed, but the vortex-shedding frequency was reduced and the base pressure was increased. Bearman<sup>3</sup> used a model with a long streamlined upstream section that terminated abruptly at a rearward-facing plane surface, to which splitter plates of different lengths were attached. Bearman found that the  $St_D$  based on the frequency of the dominant peak in the velocity spectrum varied with  $Re_D$ . Apelt et al.<sup>4</sup> studied circular cylinder wake flows with splitter plate length  $L/D = 2$  for  $Re_D = 10^4$  to  $5 \times 10^4$ . Maximum change in the base pressure drag coefficient and the wake width was observed for  $L/D = 1$ . Later, Apelt and West<sup>5</sup> extended the study of Apelt et al.<sup>4</sup> with splitter plates of  $2 \leq L/D \leq 7$ . They found that for  $L/D > 5$  vortex shedding from the cylinder was eliminated and there was no further change in the flow characteristics.

In a recent study, Mansingh and Oosthuizen<sup>6</sup> used a rectangular cylinder as a bluff body along with three splitter plates of  $L = D$ ,

2D, and 3D. In addition to the effect of splitter plate length on the flow characteristics, they studied the effect of the gap  $g$  (i.e., the distance between the trailing edge of the cylinder and the leading edge of the splitter plate). In general, with increasing  $L/D$  the minimum  $St_D$  value decreased. They also observed that for  $L/D = 3$

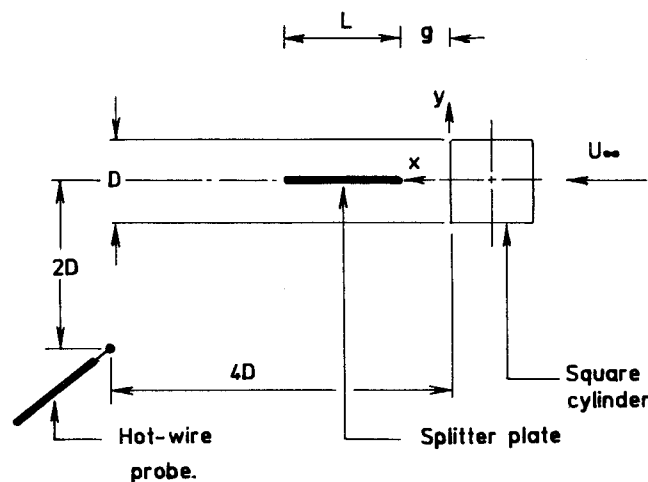


Fig. 1a Schematic of the test setup. The dimensions are not to scale.

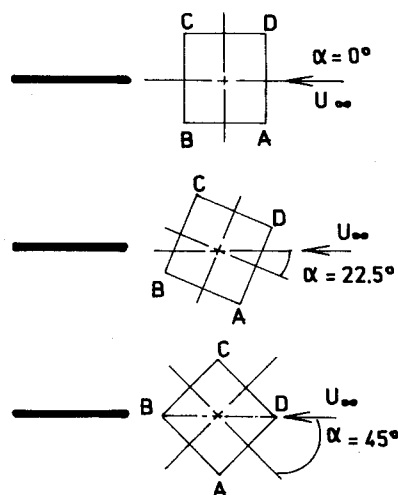


Fig. 1b Relative positions of splitter plates and square cylinder for various  $\alpha$ .

Received June 11, 1992; revision received March 15, 1994; accepted for publication March 28, 1994. Copyright © 1994 by the American Institute of Aeronautics and Astronautics, Inc. All rights reserved.

\*Associate Professor, Mechanical Engineering Department.

there was no shedding frequency for  $2 \leq g/D \leq 5$  when  $Re_D$  was greater than  $8 \times 10^2$ . Cimbalá and Garg<sup>7</sup> observed that, when allowed to rotate freely, a splitter plate shorter than five cylinder diameters does not align itself with the freestream. Instead, it migrates to a stable position on one side of the wake or the other. The splitter plate angle is a strong function of the splitter plate length but independent of the Reynolds number range tested.

These studies clearly indicate that our understanding of the cylinder wake flows in the presence of a splitter plate is far from complete. A number of important questions remain unanswered, especially the suppression of vortex formation under certain conditions. Also, the studies of Cimbalá and Garg<sup>7</sup> and of Hasan<sup>8</sup> show the importance of the angle of freestream flow  $\alpha$  to the cylinder wake development. The role of  $\alpha$  on cylinder-splitter plate flows has not been addressed.

In the present study, primary emphasis has been to study the effects of  $L/D$  and  $g/D$  on the reduction of vortex formation frequency for a square cylinder. A limited amount of data was taken with a circular cylinder to facilitate the comparison of our data with the easily available circular cylinder data in the literature. The phenomenon of inhibition of vortex shedding at certain  $L/D$  and  $g/D$  values was also addressed.

## II. Experimental Procedures

The experiment was performed in the subsonic wind tunnel at King Fahd University of Petroleum & Minerals (KFUPM). The cross section of the test section is  $1.1 \text{ m} \times 0.8 \text{ m}$ , the length being 3 m. The freestream turbulence intensity in the test section was less than 0.1%. For most of the experiments, a square Plexiglas cylinder of  $3.2 \text{ cm} \times 3.2 \text{ cm}$  was used. A circular cylinder model of diameter 3.8 cm was also used. The models spanned the 80-cm test sections, giving an  $L/D$  ratio of at least 21. The flow was found to be two dimensional at the midspan of the cylinder. The blockage ratio was less than 3%, and therefore no correction was applied to the pressure data.

The schematic of the experimental setup along with the various parameters are shown in Fig. 1a. Three splitter plates of lengths  $L = 2.9, 6.3$ , and  $16 \text{ cm}$  were used. The thickness of the splitter plates was 1.5 mm.

A mechanism at the base of the cylinder was used to set the cylinder at any desired angle of incidence with respect to the freestream velocity. Figure 1b shows the relative position of the splitter plates for various  $\alpha$ . The surface pressure was measured with 0.5-mm holes drilled around the cylinders. These holes were connected to the manometer via plastic tubes. The resolution of the pressure measurement manometer was 0.01 mbar.

The velocity data were measured with the DISA 55MO1 hot-wire anemometer system. The anemometer was operated in the constant temperature mode with 50% overheat ratio. The spectral analysis of the velocity signal was performed with a Brüel & Kjaer

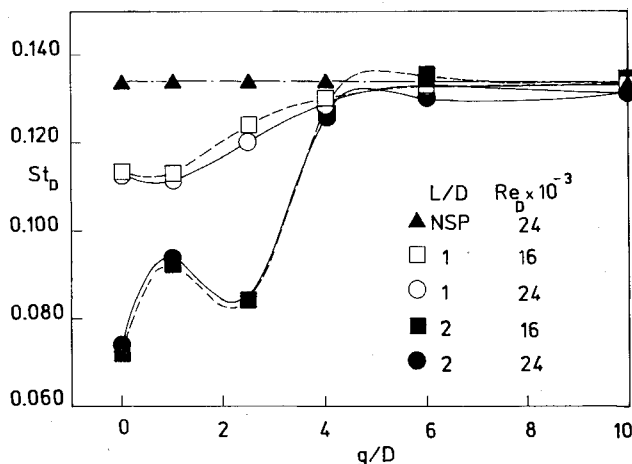


Fig. 2  $St_D$  vs  $g/D$  for square cylinder for  $\alpha = 0$ ; NSP represents "no splitter plate."

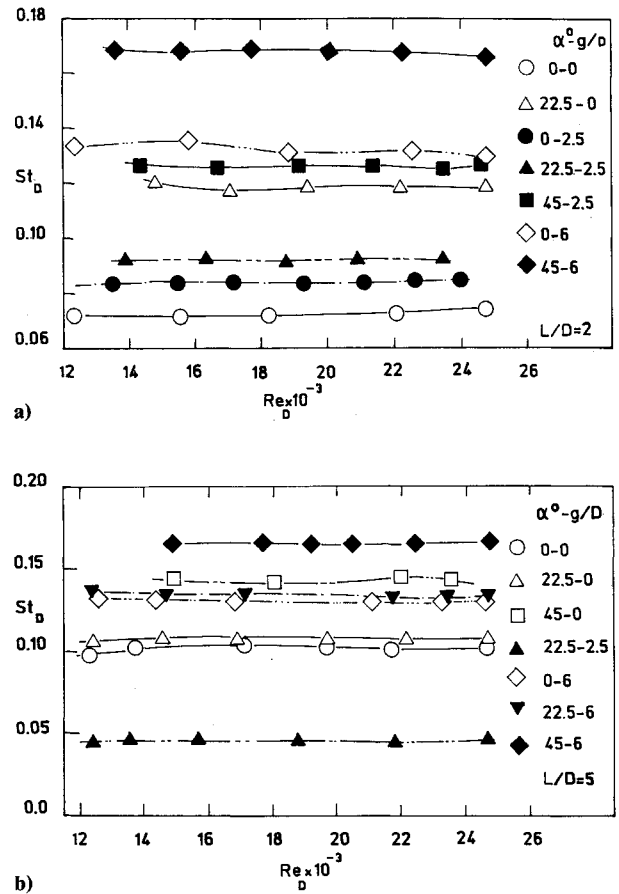


Fig. 3  $St_D$  vs  $Re_D$  for square cylinder at various  $\alpha$  and  $g/D$  values.

2033 high-resolution signal analyzer with 400 lines. Each spectrum represents the average of at least 64 instantaneous spectra.

After a number of trials, the best location for the probe was found to be at  $x = 4D$  and  $y = 2D$  for all cylinder orientations. The experiments were performed over a  $U_\infty$  range of 6–12 m/s; the corresponding  $Re_D$  range, based on the square cylinder side, was  $1.27 \times 10^4$  to  $2.54 \times 10^4$ .

The experimental uncertainty in velocity measurement was found to be less than 1%. The maximum uncertainty in the static pressure measurements was no more than  $\pm 5\%$  at the lowest velocity (6 m/s) used, whereas the same dropped below  $\pm 2\%$  at the maximum velocity (12 m/s) used.

## III. Results and Discussion

### A. Strouhal Number

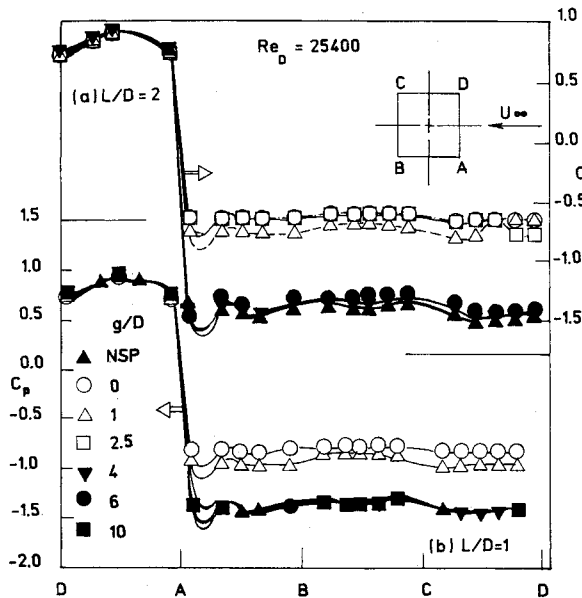
Figure 2 shows the  $St_D$  variation with  $g/D$  for the square cylinder at  $\alpha = 0$  for splitter plate lengths of  $L/D = 1$  and  $2$ , respectively. Also shown in Fig. 2 are the  $St_D$  values in the absence of a splitter plate (NSP).

The  $St_D$  values remain independent of  $Re_D$  for a fixed  $L/D$ . Without any splitter plate, the  $St_D$  value is about 0.134. The corresponding values for a rectangular cylinder<sup>6</sup> and a circular cylinder<sup>4</sup> are about 0.16 and 0.20, respectively. Note that the  $St_D$  value drops when the splitter plate is attached to the trailing edge of the cylinder, i.e.,  $g/D = 0$ . For  $L/D = 1$  and  $2$ , the  $St_D$  value drops to 0.116 and 0.071, respectively, compared with 0.134 for the cylinder alone. For  $L/D = 5$ , the corresponding value drops from 0.134 to 0.10. For  $L/D = 1$ , as  $g/D$  is increased from zero,  $St_D$  monotonically increases and reaches the asymptotic value of  $St_D = 0.134$  for the cylinder alone. For  $L/D = 2$ ,  $St_D$  shows an intermediate peak at  $g/D \approx 1$  before reaching the asymptotic value.

The drop in the  $St_D$  value due to the splitter plate is attributed to the change in the vortex formation length behind the cylinder. Gerrard<sup>9</sup> was first to suggest this explanation and was verified by Bearman,<sup>3</sup> among others.

**Table 1**  $St_D$  values for a square cylinder at various  $L/D$  and  $\alpha$  values

$L/D$	$g/D$	$St_D = fD/U_\infty$		
		$\alpha = 0$ deg	$\alpha = 22.5$ deg	$\alpha = 45$ deg
2	0	0.072	0.118	—
	2.5	0.083	0.093	0.125
	6.0	0.133	—	0.17
5	0	0.10	0.1042	0.137
	2.5	—	0.045	—
	6.0	0.127	0.128	0.157

**Fig. 4**  $C_p$  variation around square cylinder for  $\alpha = 0$  deg.

Note that Mansingh and Oosthuizen<sup>6</sup> found the  $St_D$  value to be the minimum for  $3 \leq g/D \leq 5$  for both  $L/D = 1$  and 2, unlike  $g/D = 0$  for our cases. It should be pointed out that the maximum  $Re_D$  used by Mansingh and Oosthuizen was about  $1.2 \times 10^3$ , which is significantly lower than the maximum  $Re_D$  of  $2.5 \times 10^4$  used in our experiment. They also reported no shedding frequency for  $L/D = 3$  as  $Re_D$  exceeded 800. We observed no such inhibition of vortex shedding for the whole range of Reynolds number. It suggests that the  $Re_D$  is not the proper nondimensional variable to identify the range over which the shedding frequency will be present for a cylinder with the splitter plate.

#### B. Effect of $\alpha$ on $St_D$

It has been shown by Hasan,<sup>8</sup> Lee,<sup>10</sup> and Vickery,<sup>11</sup> that the  $St_D$  value for a square cylinder without splitter plate changes with a change in the angle of attack  $\alpha$  from 0 deg. This led us to investigate the effect of  $\alpha$  on  $St_D$  values of the square cylinder with various  $L/D$  and  $g/D$  ratios.

Based on Hasan's<sup>8</sup> data, three values of  $\alpha$  (viz.,  $\alpha = 0, 22.5$ , and 45 deg) were selected to study the effect of  $\alpha$  on  $St_D$ . Figures 3a and 3b show the data for  $L/D = 2$  and 5, respectively. For a fixed  $\alpha$ , the splitter plate was moved between two and three  $g/D$  positions to measure the corresponding  $St_D$  values. This is why the data have been presented in  $St_D$  vs  $Re_D$  coordinates instead of  $St_D$  vs  $g/D$  coordinates. The results of Figs. 3a and 3b are summarized in Table 1. It can be concluded that, for any  $g/D$  value, the  $St_D$  value is the maximum for  $\alpha = 45$  deg. It also shows that, at  $\alpha = 22.5$  deg, the  $St_D$  value drops to a minimum for  $g/D = 2.5$ . The minimum value of  $St_D$  at  $\alpha = 22.5$  deg is significantly lower for  $L/D = 5$  (Fig. 3b) compared with that for  $L/D = 2$  (Fig. 3a). Note that for  $L/D = 2$  the  $St_D$  value changes from 0.072 to 0.118 as  $\alpha$  changes from 0 to 22.5 deg for  $g/D = 0$  (Fig. 3a). The corresponding change in the  $St_D$  value between  $\alpha = 0$  and 22.5 deg is insignificant for  $L/D = 5$  (Fig. 3b). Hasan<sup>8</sup> showed that for a square cylinder the vortex formation

length and the downstream distance at which the vortices from both sides of the cylinder merge are reduced significantly as  $\alpha$  is changed from 0 to 22.5 deg. A splitter plate of  $L/D \approx 2$  has minimal effect on the interaction of vortices from both sides of the cylinder. This will explain the change in the  $St_D$  value from  $\alpha = 0$  to 22.5 deg for  $L/D = 2$ . For a relatively longer splitter plate, i.e.,  $L/D = 5$  (Fig. 3b), the interaction of the vortices between the two sides of the cylinder is prevented for both  $\alpha = 0$  and 22.5 deg. Thus, very little change in  $St_D$  values is observed between these two positions of the cylinder.

The vortex-shedding characteristic of a cylinder affects the pressure distribution around the cylinder, which in turn affects the drag of the cylinder. Also, the detailed pressure distribution around the cylinder is important in understanding the flow phenomenon itself. Very few studies in the literature report pressure distribution around noncircular cylinders. These led us to document the pressure distribution around the square cylinder for various  $g/D$ ,  $L/D$ , and  $\alpha$  values at  $Re_D \approx 1.27 \times 10^4$  and  $2.54 \times 10^4$ . A few cases of these measurements are reported in the following section.

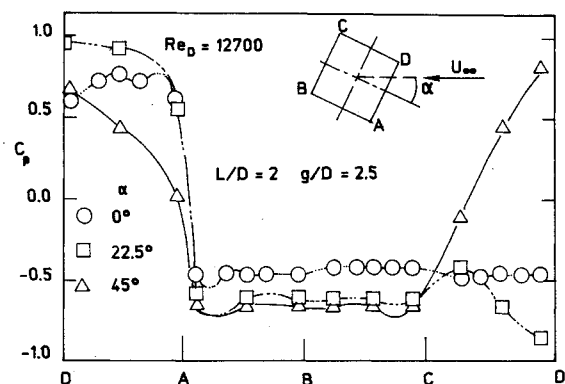
#### C. Pressure Distribution

##### 1. Square Cylinder

The pressure distribution around the cylinder is expressed in terms of the pressure coefficient  $C_p$ . For  $\alpha = 0$ , the effect of  $g/D$  on the  $C_p$  is shown in Fig. 4a for the square cylinder with  $L/D = 2$  and at a Reynolds number of  $2.54 \times 10^4$ . The corresponding data for  $L/D = 1$  are shown in Fig. 4b. The front surface of the cylinder AD shows positive  $C_p$  for all cases in Figs. 4a and 4b. This is expected, because the stagnation point is on this surface. The effect of  $Re_D$  on  $C_p$  is insignificant, and thus the data for  $Re_D = 1.27 \times 10^4$  are not shown. The  $C_p$  values for the cylinder without any splitter plate compare well with the data of Hasan.<sup>8</sup>

As the splitter plate is mounted behind the cylinder (i.e.,  $g/D = 0$ ), the average  $C_p$  value on the side and back surfaces of the cylinder changes from  $-1.40$  to about  $-0.6$  for  $L/D = 2$  (Fig. 4a). The value of  $C_p$  on the front surface remains almost constant irrespective of the splitter plate position. The  $C_p$  values on the side and back surfaces remain around  $-0.6$  for  $g/D$  up to 2.5. For  $4 \leq g/D \leq 10$ , the  $C_p$  value decreases to that for the cylinder alone. For  $0 \leq g/D \leq 2.5$ , the increase in  $C_p$  values on the surfaces BC, CD, and BA represents a reduction in the cylinder drag.

Although it has been demonstrated that the shedding frequency is inversely proportional to the vortex formation length,<sup>3,4,7,9</sup> the detailed pressure distribution around the cylinder suggests that the vortex formation length behind the cylinder is a function of the acceleration the fluid experiences as it flows around the cylinder. A splitter plate at  $0 \leq g/D \leq 3$  increases the pressure on the side surface of the cylinder, which means that the acceleration of the flow along AB and DC is less than that for the cylinder alone. Hasan<sup>8</sup> showed that as the acceleration of the flow around the cylinder decreases, the length of the vortex formation increases. This will explain the reduced Strouhal numbers in Figs. 3a and 3b for  $0 \leq g/D \leq 3$ .

**Fig. 5**  $C_p$  variation around square cylinder for different  $\alpha$  values at  $g/D = 2.5$ .

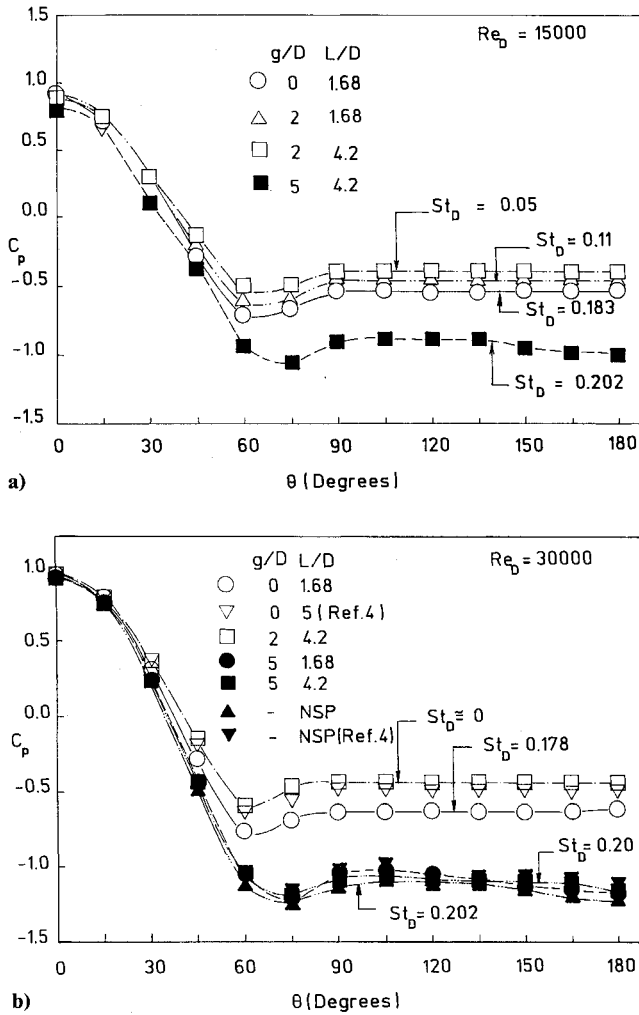


Fig. 6  $C_p$  variation around one-half of the circular cylinder.

The  $C_p$  value on the back and side surfaces of the cylinder increased from  $-1.35$  for no splitter plate to  $-1.0$  for a splitter plate of  $L/D = 1$  at  $g/D = 0$  (Fig. 4b). For  $L/D = 2$ , the corresponding change in  $C_p$  value was from  $-1.40$  to  $-0.6$  (Fig. 4a). Comparing the  $C_p$  data between  $L/D = 1$  and  $2$  for  $g/D = 0$ , one can argue that the acceleration experienced by the flow along AB and DC will be higher for  $L/D = 1$  than that for  $L/D = 2$ . Thus, the vortex formation length will be shorter and the  $St_D$  will be higher for  $L/D = 1$  compared with  $L/D = 2$ . The  $St_D$  data in Fig. 2 lend further support to the explanation relating the vortex formation length to the acceleration of the flow.

The pressure distribution around a square cylinder for various  $\alpha$  was addressed by Hasan.<sup>8</sup> The effect of a splitter plate on such pressure distribution is given later.

Figure 5 shows the pressure distribution around the square cylinder when the splitter plate of length  $2D$  is placed at  $g/D = 2.5$  and the cylinder is placed at different angle of attacks. The data are for  $Re_D \approx 1.27 \times 10^4$ . As mentioned earlier, the maximum change in  $C_p$  takes place for  $0 \leq g/D \leq 3$ . Mansingh and Oosthuizen<sup>6</sup> observed inhibition of vortex shedding at certain  $Re_D$  and  $L/D$  values when  $g/D$  was between  $2$  and  $4$ . This led us to choose  $g/D = 2.5$  for the data presented in Fig. 5. For  $\alpha = 0$  deg, the average minimum  $C_p$  value on the surfaces AB and BC is about  $-0.5$  compared with about  $-0.7$  and  $-0.75$  for  $\alpha = 22.5$  and  $45$  deg, respectively. For the cylinder alone, Hasan<sup>8</sup> found the minimum  $C_p$  value to be around  $-1.5$  and independent of  $\alpha$ . This shows that the drag reduction due to a splitter plate is also possible when the cylinder is placed at an angle with respect to the freestream velocity  $U_\infty$ .

Note that the  $C_p$  curve is nearly symmetric about point B for  $\alpha = 45$  deg. This is expected because the cylinder is symmetric about

BD line at this position. For  $\alpha = 22.5$  deg, the  $C_p$  curve oscillates on the surface CD. This implies that as the flow turns around point D toward point C, the flow separates on the surface DC before reattaching at point C. As explained earlier, the magnitude of the pressure drop affects the frequency of vortex formation. Note that the maximum drop in pressure coefficient is from  $1.0$  to  $-0.5$  for  $\alpha = 0$  deg, from  $1.0$  to  $-0.7$  for  $\alpha = 22.5$  deg, and from  $1.0$  to  $-0.75$  for  $\alpha = 45$  deg. The maximum  $C_p$  in all cases should be  $1.0$  at the stagnation point, although this is not the case in Fig. 5 due to the resolution limitation. Thus, the  $St_D$  should be the maximum for  $\alpha = 45$  deg and the minimum for  $\alpha = 0$  deg. This is consistent with the  $St_D$  values reported in Table 1 for  $g/D = 2.5$  and  $L/D = 2$ .

## 2. Circular Cylinder

A limited amount of data were taken with a circular cylinder of  $D = 3.8$  cm. Although  $C_p$  data for a circular cylinder with or without a splitter plate are available in the literature, the effect of splitter plate gap (i.e.,  $g/D \neq 0$ ) on  $C_p$  data is not available. The variation of  $C_p$  around one-half of the cylinder for different  $g/D$  values is shown in Figs. 6a and 6b for  $Re_D \approx 1.5 \times 10^4$  and  $3 \times 10^4$ , respectively. The lengths of the splitter plate used were  $6.4$  cm (i.e.,  $L/D = 1.684$ ) and  $16$  cm (i.e.,  $L/D = 4.21$ ). Figure 6b includes the data for the cylinder without a splitter plate. The  $St_D$  value corresponding to each curve in Figs. 6a and 6b is also shown in the figures. Note that the  $St_D$  value increases as the  $C_p$  minimum at the rear end of the cylinder decreases. This further strengthens our explanation regarding the relationship between  $St_D$  and the pressure distribution. In Fig. 6b, data for two cases [i.e., 1) no splitter plate and 2) splitter plate with  $L/D = 1$  and  $g/D = 0$ ] from Apelt et al.<sup>4</sup> are also included for comparison. The data without a splitter plate case show excellent agreement with the corresponding data of the

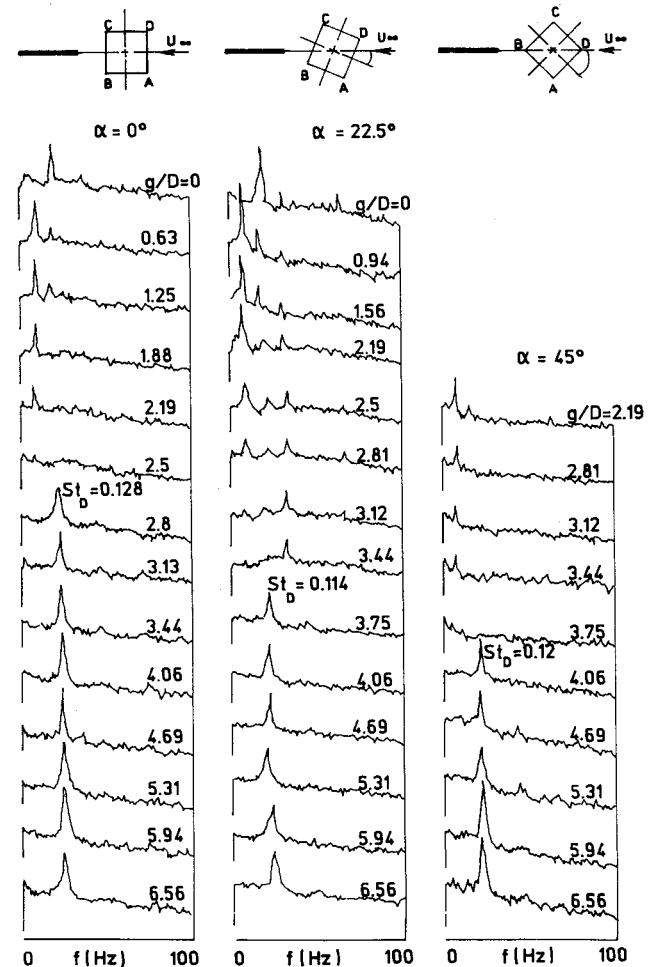


Fig. 7 The  $u$ -spectra for square cylinder at  $Re_D = 1.27 \times 10^4$  and  $L/D = 5$ .

present experiments. The second case of Apelt et al.<sup>4</sup> data represents the case for which the  $St_D$  was the minimum and the  $C_p$  value at the rear end of the cylinder was the maximum. This shows good agreement with our  $g/D = 2$  and  $L/D = 4.21$  case for which no discernible peak in the velocity spectra was observed and the negative  $C_p$  value was the maximum. The similarity of our data with those of Apelt et al. underscores the importance of another length scale in addition to the cylinder diameter in such flows.

## D. Spectral Measurements

### 1. Square Cylinder

The understanding of the disappearance or inhibition of vortex shedding in a cylinder-splitter plate flow remains incomplete in our opinion. To enhance our understanding of this important aspect of the cylinder-splitter plate flow, the longitudinal velocity spectra were measured for various  $L/D$ ,  $g/D$ , and  $\alpha$  values, varying one parameter at a time, for both the square and the circular cylinders.

Figure 7 shows the  $u$ -spectra for the square cylinder with the splitter plate of  $L/D = 5$  for three different  $\alpha$  (viz.,  $\alpha = 0, 22.5$ , and  $45$  deg) at  $Re_D \equiv 1.27 \times 10^4$ . For each  $\alpha$ , the distance between the splitter plate and the cylinder was increased in small steps to identify the range of  $g/D$  values for which the frequency peak in the spectrum disappeared. Apelt and West<sup>5</sup> reported the disappearance of shedding frequency for a circular cylinder at all velocities with a splitter plate of  $L/D \geq 5$  and  $g/D = 0$ , whereas Mansingh and Oosthuizen<sup>6</sup> found the shedding frequency of a rectangular cylinder to disappear at  $Re_D > 800$  for  $L/D = 3$ . In Fig. 7, we observe no such disappearance of the frequency peak at any  $g/D$  for all three  $\alpha$  values. A number of interesting facts can be observed in Fig. 7. First, the value of the frequency peak drops to a lower value as  $g/D$  is increased from 0; i.e., a gap is placed between the cylinder and the splitter plate. Second, the frequency value jumps back to a higher value at  $g/D \approx 2.8$  for  $\alpha = 0$  and  $22.5$  deg and at  $g/D \approx 4.0$  for  $\alpha = 45$  deg. If the projected diameter  $D_p$  (the maximum dimension of the cylinder perpendicular to the flow) of the cylinder for  $\alpha = 45$  deg is used to normalize the gap, the corresponding  $g/D_p$  value turns out to be 2.87, which is close to the value for  $\alpha = 0$  and  $22.5$  deg. No significant change in  $St_D$  was observed for  $0 < g/D < 2.8$ . Thus for  $\alpha = 45$  deg,  $g/D$  value started from 2.18.

It is clear that the  $St_D$  value jumps to a higher value between  $g/D = 2.5$  and 3. Hasan<sup>8</sup> showed that, for a square cylinder at  $\alpha = 22.5$  deg, the shear layers on each side of the cylinder behave independent of each other due to the asymmetry. We believe that this is the

reason for the multiple peaks present in the spectra up to  $g/D = 3.125$  for  $\alpha = 22.5$  deg in Fig. 7. This led us to believe that the low-frequency peaks observed for lower  $g/D$  values were due to the interaction of the shear layer with the leading edge of the splitter plate. In fact, a close inspection showed a slight decrease in the frequency with increasing  $g$  (up to  $g/D = 2.5$  for  $\alpha = 0$  deg,  $g/D = 2.18$  for  $\alpha = 22.5$  deg, and  $g/D = 3.75$  for  $\alpha = 45$  deg), which is reminiscent of the self-sustained oscillation phenomena,<sup>12-15</sup> among others. It is now a well-known fact that the self-sustained oscillation phenomenon is a shear layer instability phenomenon, supported by a feedback mechanism from the impinging edge to the upstream separation point where the disturbance is reinforced due to the phase matching. Note that the final  $St_D$  values of approximately 0.12 at high  $g/D$  values are due to the global mode of wake instability. We strongly believe that the low-frequency peaks for low  $g/D$  values are associated with the shear layer instability frequency. Careful observation shows that for low  $g/D$  values the lowest frequency peaks in Fig. 7 are the one-third harmonics of the global shedding frequency. This suggests that there is some form of coupling between the shear layer frequency and the shedding frequency of the wake for  $g/D \leq 3$ .

The coupling of two or more instability modes has been reported previously for other types of flows.<sup>12,16</sup> For  $g/D \geq 2.5$ , the influence of the shear layer on the global shedding frequency disappears.

The data with the square cylinder, as shown in Fig. 7, clearly indicate that the spectral peak is not completely inhibited for any combinations of  $L/D$  and  $g/D$ . Although for some  $L/D$  it may appear that the frequency peak is inhibited completely for certain splitter plate gaps, a closer inspection of the spectra merely reveals a switch from shear layer instability peak to global mode of wake instability. This contradicts the observation of Apelt and West,<sup>5</sup> who reported a complete inhibition of frequency peak in a circular cylinder for  $L/D = 5$ . Mansingh and Oosthuizen<sup>6</sup> reported the vortex inhibition in a rectangular cylinder for  $L/D = 3$  and  $g/D = 2.5$  for  $Re_D$  greater than 800. These discrepancies led us to study the velocity spectra for a circular cylinder as well.

### 2. Circular Cylinder

Figure 8 shows the variation of the  $u$ -spectra with  $g/D$  for three different  $L/D$  values at  $Re_D = 1.5 \times 10^4$ . For  $L/D = 0.76$ , the effect of the splitter plate on  $u$  spectra is minimal, although a jump to a higher frequency peak is clearly observed at  $g/D = 2.37$ . Also for

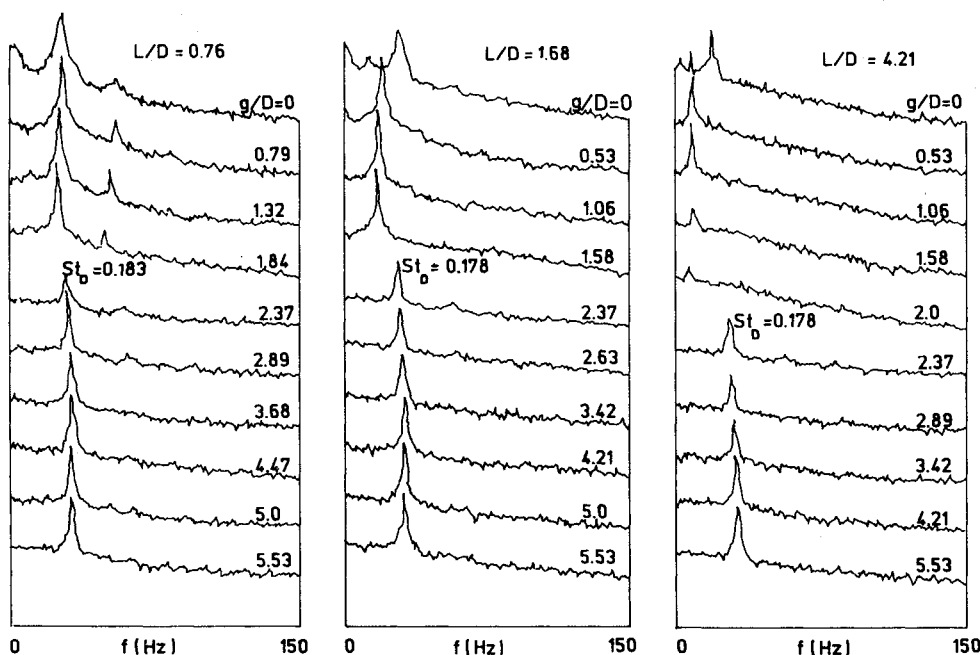


Fig. 8 The  $u$ -spectra for circular cylinder at  $Re_D = 1.5 \times 10^4$ .

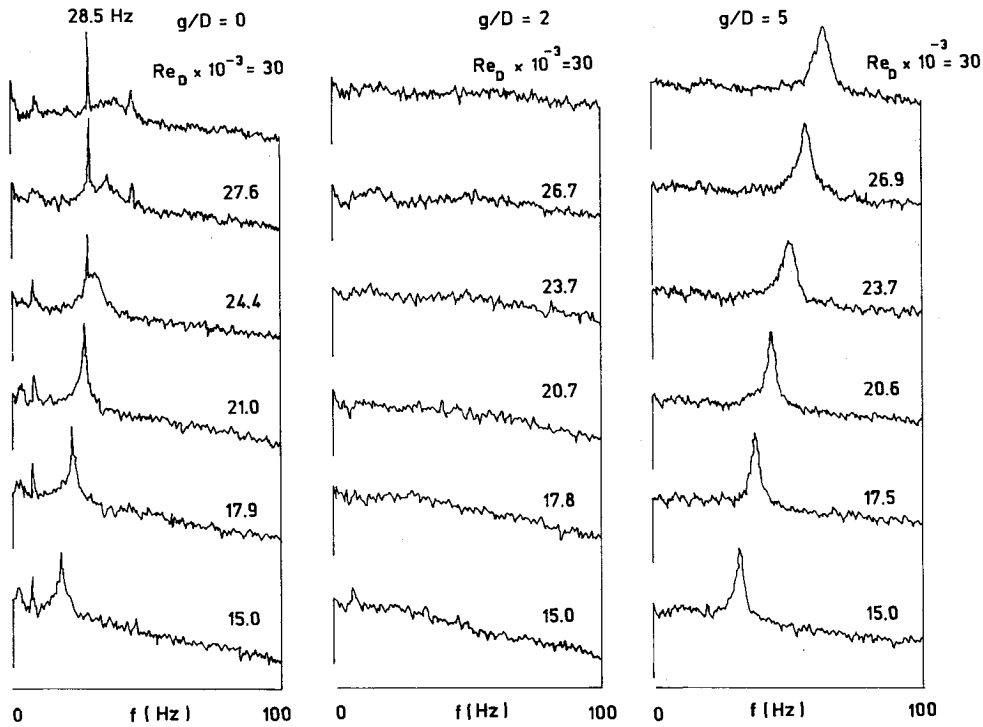


Fig. 9 Variation of  $u$ -spectra with  $Re_D$  for circular cylinder with  $L/D = 4.2$ .

$g/D < 2.37$ , the frequency of the spectral peak shows decrease with increasing  $g/D$ , which is similar to that of the square cylinder. The data at other  $L/D$  values (i.e.,  $L/D = 1.68$  and  $4.21$ ) are quite similar to their  $L/D = 0.76$  counterpart. For all three splitter plate lengths, the jump of the frequency peak at a higher Strouhal number ( $St_D \approx 0.18$ ) at around  $g/D = 2.37$  represents a switch from shear layer instability controlled frequency to global mode of shedding frequency of a wake.

In Fig. 8, a clear second peak is observed for  $L/D = 0.76$  and  $g/D \leq 1.84$ . The second peak represents the  $2f$  component. For a small splitter plate, the interaction of the vortices from the two sides of the cylinder are probably not interrupted and thus give rise to the  $2f$  component. The same is not true for the larger splitter plates of  $L/D = 1.68$  and  $4.21$ .

It should be pointed out that for  $L/D = 4.21$  the frequency peak is relatively small at  $g/D = 2$ , but it does not disappear completely as reported by others.

The effect of  $Re_D$  on the vortex formation characteristics was explored further for  $L/D = 4.21$  and is shown in Fig. 9. The sharp narrow peak at  $28.5$  Hz for  $g/D = 0$  represents the splitter plate vibration, and it started at  $Re_D = 2.44 \times 10^4$ . The splitter plate vibration was verified by an accelerometer. Other than this, the shedding frequency increased monotonically with increasing  $Re_D$ . This is also true for  $g/D = 5$ . But note that for  $g/D = 2$  no spectral peak is observed for  $Re_D > 1.5 \times 10^4$ . As the vortex formation characteristic is strongly influenced by the self-sustained shear layer instability phenomenon, it appears that at  $Re_D > 1.5 \times 10^4$ , the splitter plate spacing of  $g/D \approx 2$  prevents reinforcement of the disturbance at the separation point, and thus inhibits vortex formation. Hussain and Hasan<sup>12</sup> have shown that a self-sustained oscillation tone is not possible with a turbulent separation boundary layer unless a resonator is present in the system. Mansingh and Oosthuizen<sup>6</sup> suggested that a change in the upstream boundary-layer state is perhaps responsible for the inhibition of vortex formation at certain  $L/D$  and  $g/D$  combinations. The fact that the vortex formation, if at all, disappears only over a very small range of  $g/D$  values for the whole range of  $Re_D$  appears to suggest that the phenomenon is not strictly dependent on the state of the separation boundary layer. We believe that the disappearance of the vortex formation at certain  $g/D$  values is due to the cancellation rather than reinforcement

of the upstream disturbance due to the feedback cycle. Detailed phase measurements will be necessary to establish the proposed hypothesis. Such phase measurements are outside the scope of the present work.

#### IV. Conclusions

The flow over different cylinders in the presence of splitter plates of various lengths was experimentally studied over a  $Re_D$  range of  $1.2 \times 10^4$  to  $3 \times 10^4$ . Most of the data were taken for a square cylinder, whereas a limited amount of data were taken for a circular cylinder.

The  $St_D$  value due to the frequency representing the spectral peak decreased when a splitter plate was placed behind the cylinder at  $g/D \leq 3$ . This peak is probably associated with the shear layer instability frequency. For  $g/D \geq 4$ , the frequency of the spectral peak increased back to the original value of the global shedding frequency. This suggests that the influence of the splitter plate on the shedding characteristics of the cylinder disappears for  $g/D \geq 4$ . The detailed pressure distribution suggested that the amount of pressure drop around the cylinder and thus the acceleration of the flow can be used to predict the qualitative variation of the  $St_D$  with increasing gap between the cylinder and the splitter plate. The qualitative variation of the  $St_D$  with  $g/D$  remains unchanged with a change in the direction of incidence flow.

Spectral measurements suggested for the first time that for a small  $g/D$  the shear layer instability tone played a role in controlling the frequency characteristic of a cylinder flow. For large  $g/D$ , the shear layer instability tone was not there, and only the wake instability was present. A tentative explanation has been provided for the inhibition of the vortex formation phenomenon as reported by others.

Future studies should look into the downstream phase distribution as a function of  $L/D$  and  $g/D$  to establish the exact nature of the feedback cycle at work and also to explain the inhibition of vortex formation provided it is there.

#### Acknowledgement

The authors would like to thank King Fahd University of Petroleum & Minerals for supporting the research.

## References

- <sup>1</sup>Roshko, A., "On the Drag and Shedding Frequency of Two-Dimensional Bluff Bodies," NACA TN 3169, 1954.
- <sup>2</sup>Roshko, A., "On the Wake and Drag of Bluff Bodies," *Journal of Aeronautical Sciences*, Vol. 22, 1955, pp. 124-137.
- <sup>3</sup>Bearman, P. W., "Investigation of the Flow Behind a Two-Dimensional Model with a Blunt Trailing Edge and Fitted with Splitter Plates," *Journal of Fluid Mechanics*, Vol. 21, Pt. 2, 1965, pp. 241-255.
- <sup>4</sup>Apelt, C. J., West, G. S., and Szweczyk, A. A., "The Effects of Wake Splitter Plates on the Flow Past a Circular Cylinder in the Range  $10^4 < Re < 5 \times 10^4$ ," *Journal of Fluid Mechanics*, Vol. 61, Oct. 1973, pp. 187-198.
- <sup>5</sup>Apelt, C. J., and West, G. S., "The Effects of Wake Splitter Plates on Bluff-Body Flows in the Range  $10^4 < Re < 5 \times 10^4$ —Part 2," *Journal of Fluid Mechanics*, Vol. 71, Pt. 1, 1975, pp. 145-160.
- <sup>6</sup>Mansingh, V., and Oosthuizen, P. H., "Effects of Splitter Plates on the Wake Flow Behind a Bluff Body," *AIAA Journal*, Vol. 28, No. 5, 1990, pp. 778-783.
- <sup>7</sup>Cimbala, J. M., and Garg, S., "Flow in the Wake of a Freely Rotatable Cylinder with Splitter Plate," *AIAA Journal*, Vol. 29, No. 6, 1991, pp. 1001-1003.
- <sup>8</sup>Hasan, M. A. Z., "The Near Wake Structure of a Square Cylinder," *International Journal of Heat & Fluid Flow*, Vol. 10, No. 4, 1989, pp.

339-348.

<sup>9</sup>Gerrard, J. H., "The Mechanics of the Formation Region of Vortices Behind Bluff Bodies," *Journal of Fluid Mechanics*, Vol. 25, Pt. 3, 1966, pp. 401-413.

<sup>10</sup>Lee, B. E., "The Effect of Turbulence on the Surface Pressure Field of a Square Prism," *Journal of Fluid Mechanics*, Vol. 69, Pt. 2, 1975, pp. 263-282.

<sup>11</sup>Vickery, B. J., "Fluctuating Lift and Drag on a Long Cylinder of Square Cross-Section in a Smooth and in a Turbulent Flow," *Journal of Fluid Mechanics*, Vol. 25, Pt. 3, 1966, pp. 481-494.

<sup>12</sup>Hussain, A. K. M. F., and Hasan, M. A. Z., "The Whistler Nozzle Phenomenon," *Journal of Fluid Mechanics*, Vol. 134, 1983, pp. 431-458.

<sup>13</sup>Knisely, C., and Rockwell, D., "Self-Sustained Low-Frequency Components in an Impinging Shear Layer," *Journal of Fluid Mechanics*, Vol. 116, 1982, pp. 157-186.

<sup>14</sup>Chanaud, R. C., and Powell, A., "Some Experiments Concerning the Hole and Ring Tone," *Journal of the Acoustical Society of America*, Vol. 37, 1965, pp. 902-911.

<sup>15</sup>Sarohia, V., "Experimental Investigation of Oscillations in Flows Over Shallow Cavities," *AIAA Journal*, Vol. 15, No. 7, 1977, pp. 984-991.

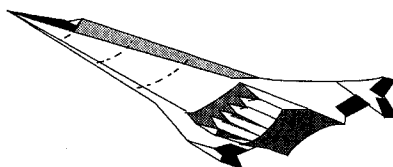
<sup>16</sup>Gharib, M., and Roshko, A., "The Effect of Flow Oscillations on Cavity Drag," *Journal of Fluid Mechanics*, Vol. 177, April 1987, pp. 501-530.

*Fills the gaps in hypersonic literature with two self-contained, comprehensive volumes*

## Hypersonic Airbreathing Propulsion

William H. Heiser and David T. Pratt

Developed through course work at the Air Force Academy, and supported through funding by the NASP program and Wright Laboratory, this new text emphasizes fundamental principles, guiding concepts, and analytical derivations and numerical examples having clear, useful, insightful results. *Hypersonic Airbreathing Propulsion* is completely self-contained, including an extensive array of PC-based, user friendly computer programs that enable the student to reproduce all results. Based on a great deal of original material, the text includes over 200 figures and 130 homework examples. Physical quantities are expressed in English and SI units throughout.



1994, 594 pp, illus, Hardback, ISBN 1-56347-035-7  
AIAA Members \$69.95, Nonmembers \$89.95  
Order #: 35-7(945)

## Hypersonic Aerothermodynamics

John J. Bertin

The first four chapters present general information characterizing hypersonic flows, discuss numerical formulations of varying degrees of rigor in computational fluid dynamics (CFD) codes, and discuss the strengths and limitations of the various types of hypersonic experimentation. Other chapters cover the stagnation-region flowfield, the inviscid flowfield, the boundary layer, the aerodynamic forces and moments, viscous/inviscid interactions and shock/shock interactions, and a review of aerothermodynamics phenomena and their role in the design of a hypersonic vehicle. Sample exercises and homework problems are presented throughout the text.

1994, 610 pp, illus, Hardback, ISBN 1-56347-036-5  
AIAA Members \$69.95, Nonmembers \$89.95  
Order #: 36-5(945)

Place your order today! Call 1-800/682-AIAA



American Institute of Aeronautics and Astronautics

Publications Customer Service, 9 Jay Gould Ct., P.O. Box 753, Waldorf, MD 20604  
FAX 301/843-0159 Phone 1-800/682-2422 8 a.m. - 5 p.m. Eastern

Sales Tax: CA residents, 8.25%; DC, 6%. For shipping and handling add \$4.75 for 1-4 books (call for rates for higher quantities). Orders under \$100.00 must be prepaid. Foreign orders must be prepaid and include a \$20.00 postal surcharge. Please allow 4 weeks for delivery. Prices are subject to change without notice. Returns will be accepted within 30 days. Non-U.S. residents are responsible for payment of any taxes required by their government.